

Received July 12, 2021; reviewed; accepted September 11, 2021

## Citric acid inhibits the floatability of quartz in the $Mg^{2+}$ system

Yonglun Wang<sup>1,2</sup>, Jie Li<sup>1</sup>, Wenhao Zhang<sup>1,2</sup>, Pengwei Li<sup>1,2</sup>, Jing Guo<sup>1,2</sup>, Kai Yao<sup>1,2</sup>

<sup>1</sup> School of Materials and Metallurgy, Inner Mongolia University of Science and Technology, Baotou, 014010, China

<sup>2</sup> School of Mining and Coal, Inner Mongolia University of Science and Technology, Baotou, 014010, China

Corresponding author: yjslijie@sohu.com (Jie Li)

**Abstract:** Citric acid is a small-molecule organic acid, which can be used as an inhibitor for the flotation of  $Mg^{2+}$  activated quartz. Methods such as flotation experiments, zeta potential, FTIR qualitative and quantitative calculations, and solution chemistry calculations were used in this study to conduct systematic research to study activation and inhibition mechanisms.

The results show that adding only a quarter of citric acid under the optimal conditions of  $Mg^{2+}$  activated quartz produces the best inhibitory effect.  $Mg^{2+}$  and citric acid affect the zeta potential of the quartz surface in the zeta potential experiment. FTIR qualitatively found that under the action of  $Mg^{2+}$ , sodium oleate was adsorbed on the quartz surface in the form of physical adsorption; quantitative analysis clearly explained that after the chemical reaction between citric acid and  $Mg^{2+}$ , it desorbed from the quartz surface into the water system. According to the chemical calculation of the solution during the flotation process, it is found that the reaction product of citric acid and  $Mg^{2+}$  has no inhibitory effect; only the amount of  $Mg^{2+}$  is consumed, thereby reducing the number of activating factors and cutting off the medium of sodium oleate adsorbed on the surface of the quartz.

**Keywords:** quartz, activate, inhibit, physical adsorption, quantitative infrared spectroscopy

### 1. Introduction

When minerals, such as quartz, co-occurring soluble aluminum and magnesium salts are floated, the inevitable ions ( $Ca^{2+}$ ,  $Mg^{2+}$ ,  $Fe^{3+}$ ,  $Al^{3+}$ , etc.) are formed by the dissolution of minerals in the slurry. These unavoidable ions will continue to accumulate in the process of circulating water in the beneficiation plant. When the ion concentration reaches a particular level, the ions will activate the quartz in the flotation, causing the anion collector to become adsorbed on the quartz and enter the concentrate with the foam, lowering the grade of the concentrate. Recently, the application of nonmetallic materials has become more widespread, and quartz has become an important role in nonmetallic materials. Positive flotation procedures include using cationic collectors to enrich quartz or using metal cation activation first and then anionic collectors to finish the flotation. In addition, the reverse flotation process can be used to remove impurities from quartz. It is necessary to use inhibitors to inhibit quartz and increase the recovery rate quartz.

There are numerous studies on quartz activation globally (Zhang 2019; Ji et al., 2021). Yin et al. (Yin et al., 2013) used SAS as a collector and  $Mg^{2+}$  as an activator to study the mechanism of  $Mg^{2+}$  activated quartz flotation. Fuerstenau et al. (Fuerstenau et al., 1989) found that the monovalent hydroxyl metal complex is the major component of activated quartz flotation. Wu et al. (Wu et al. 2007) used  $Fe^{3+}$  to activate quartz. Under medium alkaline conditions, formed hydroxide precipitated activated quartz, and used oxalic acid, EDTA, citric acid, etc. 5 kinds of organic chelating agents are used as flotation inhibitors the inhibition mechanism of organic chelation agents has been studied.

In this study,  $Mg^{2+}$  is used as an activator to activate quartz, and citric acid is used as an inhibitor to inhibit quartz activated by  $Mg^{2+}$ . Sodium oleate is used in flotation experiments as a collector. Later, the phenomenon of flotation will be explained using instrument characterization and calculation.

## 2. Materials and methods

### 2.1. Materials

Quartz minerals were taken from the Inner Mongolia. Pure quartz minerals of  $-74\ \mu\text{m}$  accounting for 97.64% were obtained as experimental raw materials after ultrasonic cleaning, crushing, hand-selection, grinding, sieving, and pickling. After X-ray fluorescence detection, the multi-element analysis results of pure quartz minerals are obtained (Table 1.1), in which the concentration of  $\text{SiO}_2$  is more than 99%, which is used as the raw material for the flotation test of pure quartz minerals.

Table 1. Chemical composition content of quartz

Element	$\text{SiO}_2$	$\text{Al}_2\text{O}_3$	$\text{Fe}_2\text{O}_3$	CaO	BaO	$\text{Cr}_2\text{O}_3$	NiO
Wt. %	99.7973	0.0675	0.0564	0.0430	0.0233	0.0098	0.0027

Experimental reagents: Sodium oleate (AR), magnesium chloride (AR), citric acid (AR), hydrochloric acid, sodium hydroxide, all analytical grade. During the experiment, both the configuration solution and the test water were deionized water.

Experimental equipment: XFG hanging tank flotation machine ( $50\ \text{cm}^3$ ), Brookhaven Zeta potentiometer, Bruker VERTEX70 Fourier infrared spectrometer, electronic balance, centrifuge, magnetic stirrer, etc.

### 2.2. Methods

#### 2.2.1. Flotation test

XFG hanging trough flotation machine (Jilin Province Prospecting Plant) was used for flotation experiment. The flotation trough volume was  $50\ \text{cm}^3$ , 4g quartz pure minerals were added each time, and the slurry concentration was 8%. Adjust the slurry the pH with hydrochloric acid or sodium hydroxide for 1 min, stir for 2 min, add  $\text{Mg}^{2+}$  and stir for 3 min, add collectors then continue stirring for 3 min, turn on the inflation function, perform bubble scraping, and after scraping for 3 min, separate the foam product and the bottom product are dehydrated, dried and weighed at  $38^\circ\text{C}$ , and the flotation recovery rate is calculated. Three parallel experiments are performed to avoid the human error caused by manual foam scraping, and the average of the three experimental results is taken. The experimental process is shown in Fig. 1

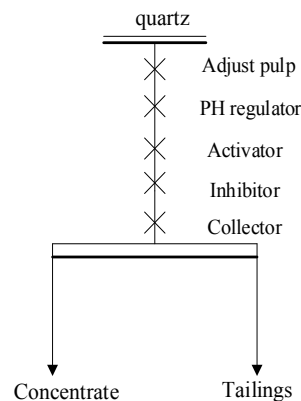


Fig. 1. Flow chart of flotation test

#### 2.2.2. Zeta potential

Take an appropriate amount of pure quartz and grinding it to  $-20\ \mu\text{m}$  in a mortar, and weigh 0.2g of pure quartz, add a certain amount of water and medicament, adjust to the specified pH value, stir with a magnetic stirrer, and after sufficient sedimentation, extract the supernatant and measures the zeta potential using the zeta potentiometer (Brookhaven).

### 2.2.3. FTIR spectra measurement

Under different experimental conditions, the Bruker VERTEX70 Fourier infrared spectrometer is used to detect the collector's adsorption on the quartz surface. When pH = 10, the concentration of  $Mg^{2+}$  is  $1 \times 10^{-3}$  mol/L, citric acid (CA) is  $1 \times 10^{-4}$  mol/L, and the concentration of sodium oleate is 120 mg/L. Prepare the test sample, and mix the sample with potassium bromide in a ratio of 1:150. The spectral parameters are  $400\text{--}4000\text{ cm}^{-1}$ , and the resolution is  $1\text{ cm}^{-1}$  (Liu et al., 2020).

## 3. Results and discussion

### 3.1. Flotation test

#### 3.1.1. Influence of pulp pH on flotation

The influence of pulp pH on the recovery rate of quartz flotation was investigated under the conditions of  $Mg^{2+}$  concentration of  $1.0 \times 10^{-3}$  mol/L and Na-OL concentration of 100 mg/L, and the results are shown in Fig. 2. As shown in Fig. 2, the flotation recovery rate of pure quartz is below 10% when the pH is between 2 and 14. After adding  $Mg^{2+}$ , under acidic pH < 7, the recovery rate is similar to that without  $Mg^{2+}$ . However, when pH > 7, the recovery rate rises rapidly, and when pH = 10, the recovery rate reaches 82.9%. As the pH continues to grow, the recovery rate begins to show a downward trend.

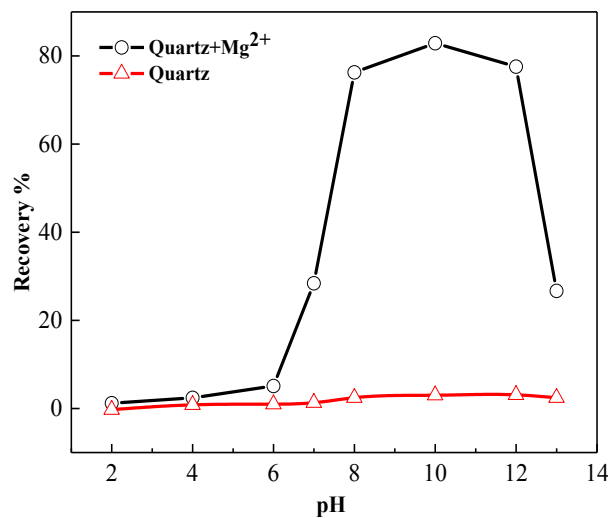


Fig. 2. Effect of pH value on flotation

#### 3.1.2. Influence of $Mg^{2+}$ concentration on the flotation recovery rate

When the pulp pH = 10, the recovery rate reaches its maximum value in the pulp pH experiment. Therefore, under the condition of pH 10, the relationship between the amount of  $Mg^{2+}$  and the recovery rate of quartz flotation is explored. The experimental results are presented in Fig. 3. When the concentration of  $Mg^{2+}$  is  $1 \times 10^{-5}$  mol/L, the flotation recovery rate is 24.6%. Compared with no  $Mg^{2+}$ , the flotation recovery rate is enhanced by 20.62% under the same conditions. As the concentration of added  $Mg^{2+}$  increases, the flotation recovery rate shows an upward trend, and when the  $Mg^{2+}$  concentration is  $1 \times 10^{-3}$  mol/L, the flotation recovery rate gets to the maximum. When  $Mg^{2+}$  increased to 0.1 mol/L, the flotation recovery rate slowly decreased.

Due to the electrostatic attraction between  $Mg^{2+}$  and the quartz surface, the negatively charged area of  $Mg^{2+}$  is adsorbed on the quartz surface, resulting in a positively charged area where the quartz surface adsorbs  $Mg^{2+}$  (Zhang et al., 2019). When sodium oleate is introduced, the sodium oleate component is adsorbed on these positive electric areas. However, when the concentration of  $Mg^{2+}$  is too high, OL combines with  $Mg^{2+}$  to form magnesium oleate precipitation, which consumes collectors and reduces the flotation recovery rate (Ji et al., 2021). There is also a theory that metal hydroxides generated under alkaline conditions will inhibit the floatability of minerals, which is the cause of the decrease in the recovery rate.

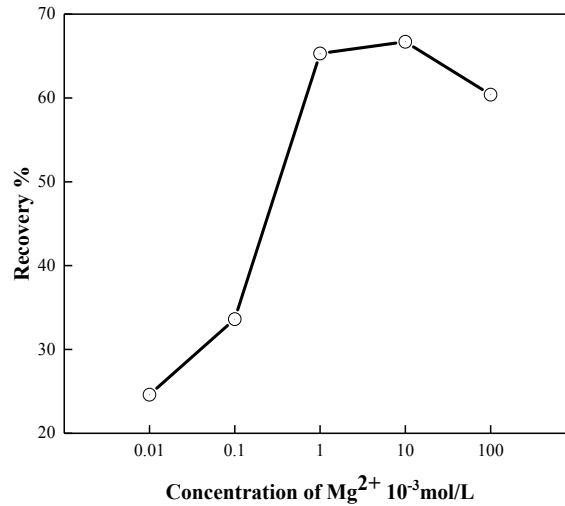


Fig. 3. Effect of  $Mg^{2+}$  concentration on flotation

### 3.1.3. Influence of sodium oleate concentration on the flotation recovery rate

The optimal experimental conditions for  $Mg^{2+}$  activated quartz, based on the above experimental results, are  $pH = 10$ ,  $Mg^{2+}$  concentration of  $1 \times 10^{-3}$  mol/L. Examine the effect of Na-OI concentration on the recovery rate of quartz flotation under these conditions, and the results are shown in Fig. 4.

When the Na-OI concentration is between 60 and 120 mg/L, the flotation recovery rate gradually increases as the Na-OI concentration increases. When the collector Na-OI concentration reaches 120 mg/L, the quartz flotation recovery rate tends to be stable. And when the Na-OI concentration is 120 mg/L, the flotation recovery rate reaches the maximum.

The main reasons are as follows: The activation point of  $Mg^{2+}$  is required for Na-OI to be adsorbed on quartz. The activation points of  $Mg^{2+}$  is required for Na-OI to be adsorbed on quartz. The activation point provided by  $Mg^{2+}$  is limited, so the adsorption capacity of Na-OI is also limited. When the amount of Na-OI adsorption is saturated, the hydrophobicity of quartz reaches the highest level, and the concentration of Na-OI continues to increase, and the flotation recovery rate will no longer increase.

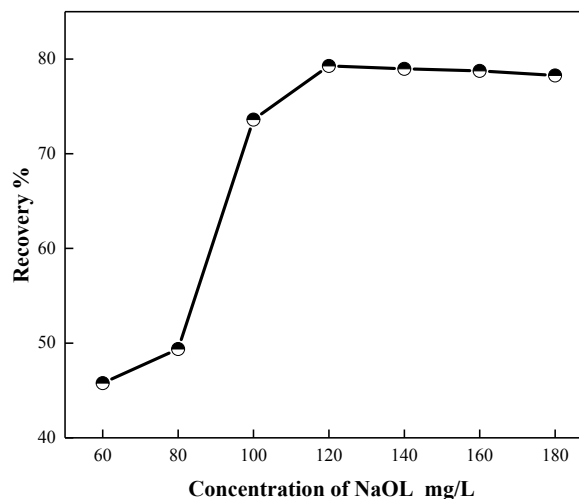


Fig. 4. Effect of Na-OI concentration on the flotation

### 3.1.4 Citric acid concentration inhibition experiment

The flotation recovery rate of quartz achieves the optimum value when  $\text{pH} = 10$ ,  $\text{Mg}^{2+}$  concentration is  $1 \times 10^{-3}$  mol/L, and sodium oleate concentration is 120 mg/L. Under these conditions, the inhibitory effect of CA on quartz flotation was studied, and the experimental results are shown in Fig. 5.

The pH of the pulp is measured after CA is introduced to ensure that the pH of the pulp does not vary greatly as a result of the addition of CA, which could alter the experimental circumstances. As a result, the CA concentration range chosen is  $0\text{--}3.5 \times 10^{-4}$  mol/L.

Under the above conditions, when the concentration of CA reaches  $2.5 \times 10^{-4}$  mol/L, the flotation recovery rate of quartz is lower than 10%. The recovery rate no longer decreases with the increase in CA, but it tends to be stable. Therefore, when the concentration of CA is  $2.5 \times 10^{-4}$  mol/L, the inhibition of  $\text{Mg}^{2+}$  activated quartz has reached the best state, and the flotation recovery rate is lower than that of pure quartz flotation. The most likely reason is that other metal impurities activate the quartz with 99% raw material purity. The activation factor of this part is also inhibited by CA, resulting in a lower flotation recovery rate.

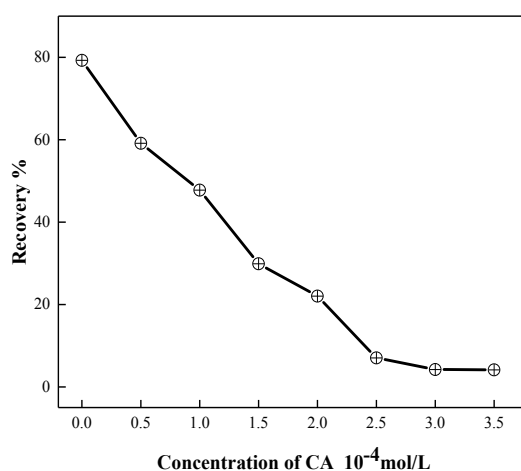


Fig. 5. Effect of CA concentration on the flotation

### 3.2. Zeta potential analysis

As shown in Fig. 6, when  $\text{Mg}^{2+}$  is not added, due to the fragmentation of the quartz silicon-oxygen tetrahedral lattice, the surface of the quartz exposes the broken Si-O bond and adsorbs and locates the ion  $\text{OH}^-$ , which makes the surface of the quartz negatively charged. As an anion collector, sodium oleate cannot be adsorbed on the surface of the quartz, where it has no effect.

When  $\text{Mg}^{2+}$  is added, the zeta potential value of quartz is significantly increased due to the counter-charged ions of  $\text{Mg}^{2+}$  and the hydroxyl complex. Around  $\text{pH} = 10$ , the zeta potential of quartz surface changes to a positive value. Metal cations and hydroxyl complexes act on the surface of the quartz, and the number of activation points is the largest, providing action points for sodium oleate. This is consistent with the result that the flotation recovery rate reaches the highest value at  $\text{pH} = 10$  during the flotation experiment.

But as the pH continued to grow,  $\text{Mg}^{2+}$  produced hydroxide precipitates, and the zeta potential dropped to a negative value. After adding  $\text{Mg}^{2+}$  and CA, when the  $\text{pH} > 7$ , the zeta potential of the quartz surface will also increase. However, due to the chemical reaction between CA and  $\text{Mg}^{2+}$ , water-soluble products are formed. The number of cations and hydroxyl complexes adsorbed on the quartz surface decreases, and the value cannot be changed to a positive value.

### 3.3. FTIR Qualitative analysis

Infrared spectroscopy was used to examine four samples: quartz + sodium oleate, quartz +  $\text{Mg}^{2+}$  + sodium oleate, and quartz +  $\text{Mg}^{2+}$  + CA + sodium oleate. The spectrum is shown in Fig. 7.

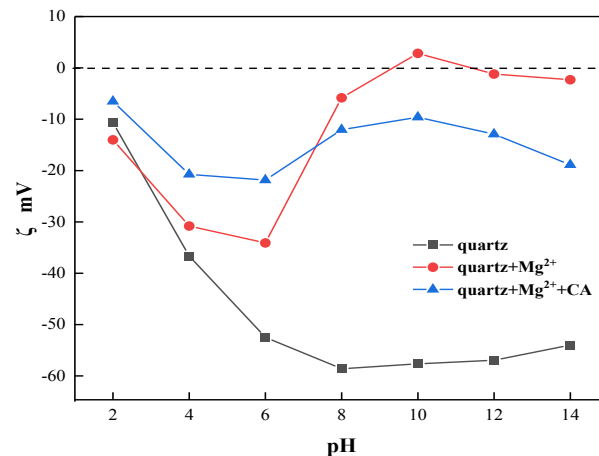


Fig. 6. Zeta potential diagram

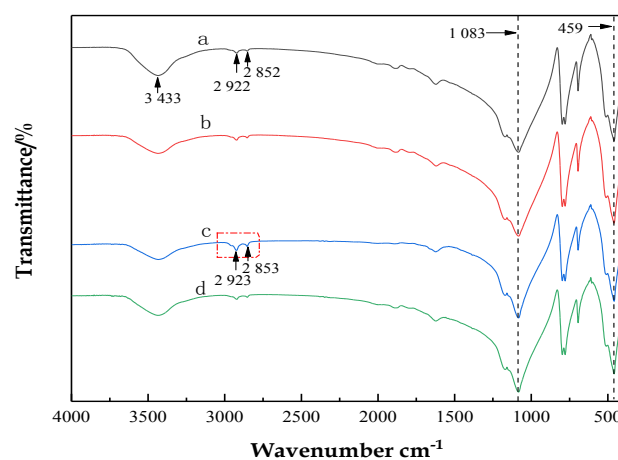
a-quartz b-quartz +Na-OI c-quartz+Mg<sup>2+</sup>+ Na-OI d-quartz+Mg<sup>2+</sup>+ CA +Na-OI

Fig. 7. Infrared spectrum of the interaction between quartz and medicament

The two absorption peaks produced by the -CH<sub>3</sub> and -CH<sub>2</sub>- functional groups in the residual organic impurities during the purification of spectrally pure potassium bromide are in Fig. 7, 2922 cm<sup>-1</sup> and 2852 cm<sup>-1</sup>. Simultaneously, these two absorption peaks are used to determine whether sodium oleate is adsorbed on quartz. Therefore, in the experiment, the ratio of potassium bromide carrier to the sample can be quantitatively matched, and the intensity of the absorption peak can be used for qualitative analysis.

Curve a shows the strong and broad absorption peak of Si-O-Si antisymmetric stretching vibration at 1083 cm<sup>-1</sup> in the infrared spectrum of quartz; 798 cm<sup>-1</sup> and 779 cm<sup>-1</sup> represent Si-O-Si stacking and stretching. Vibration splitting produces two absorption peaks: 459 cm<sup>-1</sup> is the Si-O symmetrical variable-angle vibration absorption peak, and 459 cm<sup>-1</sup> is the Si-O symmetrical variable-angle vibration absorption peak (Weng et al., 2010).

The infrared spectrum after quartz + sodium oleate action is seen in curve b. There is no absorption peak corresponding to sodium oleate in comparison to curve a, indicating that sodium oleate is not adsorbed on the quartz surface.

The spectrum after the action of quartz + Mg<sup>2+</sup> + sodium oleate is represented by curve c. The -CH<sub>2</sub>- stretching vibration absorption peak of sodium oleate is found at 2923 cm<sup>-1</sup>, whereas the -CH<sub>3</sub> stretching vibration peak is found at 2853 cm<sup>-1</sup>. It is thought that sodium oleate can be adsorbed on the quartz surface after Mg<sup>2+</sup> activation. However, there is no noticeable wavenumber redshift in the corresponding peak position when quartz adsorbs the drug. At 2853 cm<sup>-1</sup> and 2923 cm<sup>-1</sup>, the offset is only 1 cm<sup>-1</sup>. As a result, sodium oleate adsorption on the surface of activated quartz is purely physical, with chemical adsorption having no effect.

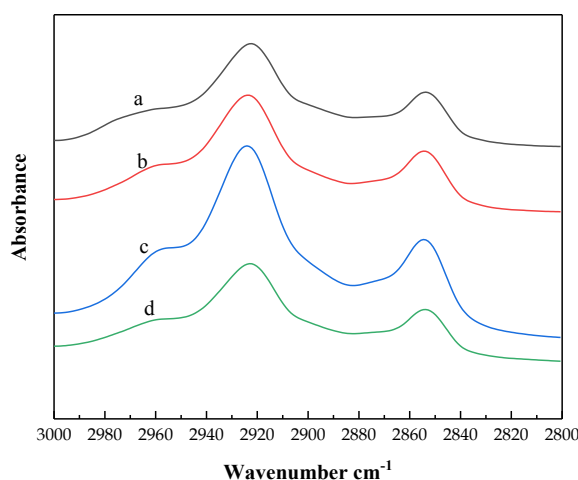
Curve d is the infrared spectrum of the interaction with sodium oleate after inhibition by CA. Compared with curve c, the absorption peak intensity of  $-\text{CH}_2-$  and  $-\text{CH}_3$  of sodium oleate is significantly reduced. This means that the  $-\text{CH}_3$  absorption peak in CA does not appear. The product of the reaction between CA and  $\text{Mg}^{2+}$  is not adsorbed on the surface of the quartz, and sodium oleate is not adsorbed on the surface of the quartz.

### 3.4. FTIR Quantitative analysis

Since it is impossible to more intuitively observe the change in the adsorption amount of sodium oleate on the quartz surface due to residual organic impurities in the purification process of spectrally pure potassium bromide, the quantitative calculation method of infrared spectroscopy (Liu et al., 2017) is used to calculate the adsorption amount of sodium oleate.

The absorption intensity of light of any wavelength is proportional to the concentration of each component in the sample and proportionate to the optical path length (sample thickness) according to the Lambert-Beer law (Weng et al., 2010). The absorption intensity is solely proportionate to the concentration since the pressure of each pressed sheet is the same as the mass and ratio of the sample and carrier used, and the thickness of all the sample sheets is uniform.

Use infrared OPUS software to convert infrared transmission spectrum (TR) into infrared absorption spectrum (AB), and perform signal smoothing processing on AB spectrum multiple times to obtain smooth infrared absorption spectrum (AB), intercept the part of  $2800\text{--}3000\text{ cm}^{-1}$ , as shown in Fig.8 Smooth infrared absorption spectrum (AB).

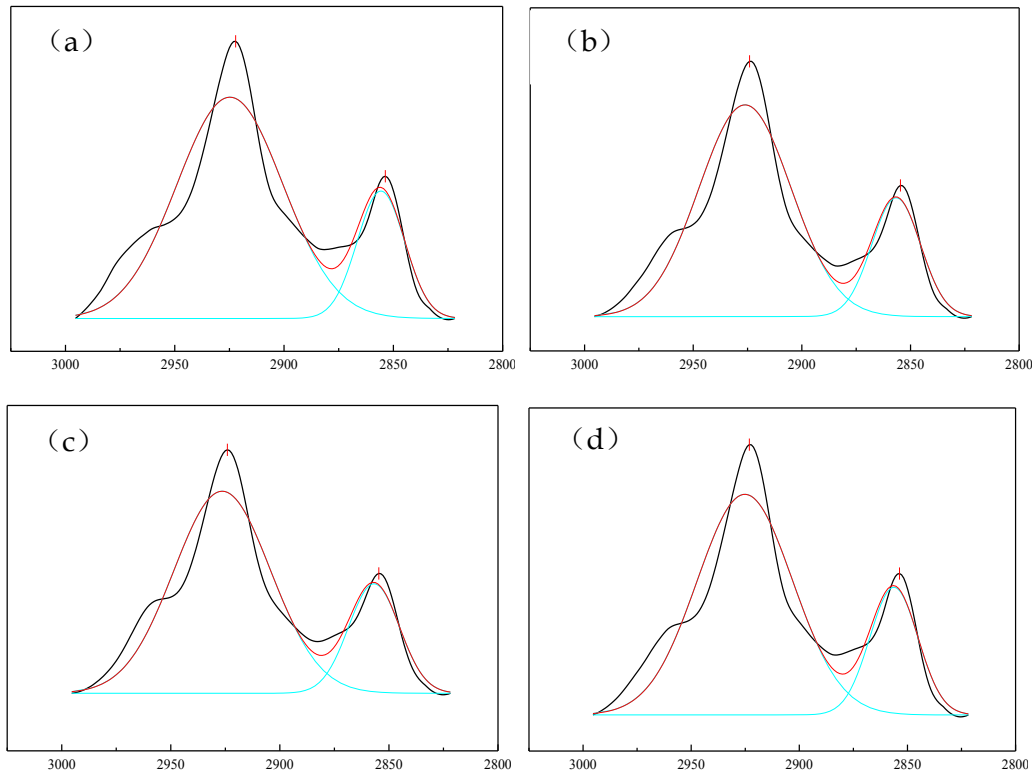


a-quartz b-quartz+Na-Ol c-quartz+ $\text{Mg}^{2+}$ + Na-Ol d-quartz+ $\text{Mg}^{2+}$ + CA +Na-Ol

Fig. 8. Smooth infrared absorption spectrum

The sub-peaks of the four smoothed spectra of a, b, c, and d are distributed using the Gaussian function. The peak fitting analysis is used in the fitting process in the Origin 2017 software. Within the provided wavenumber range, the baseline is chosen. To determine the peak area in the smoothed and fitted spectrum and compare changes in adsorption capacity, the Levenberg–Marquardt optimization approach is used: Fig. 9 shows the smooth fitting spectrum, and Table 2 shows the fitting result data.

Compared with the results of quantitative infrared spectroscopy calculations in Table 2, the peak area of a group can indicate the residual organic impurities in potassium bromide and the amount of organic matter in the raw quartz ore. In group b, sodium oleate alone interacts with quartz compared with a group a, and the peak area only increases 3.52%, indicating that only a very small amount of sodium oleate is adsorbed on the quartz. The peak area of quartz in group c was the largest after  $\text{Mg}^{2+}$  activation, and the peak area in group d was the smallest after CA inhibition. The adsorption capacity of sodium oleate in group c increased by 17.89%. The adsorption capacity of sodium oleate in group d was reduced by 24.35%, which was 35.83% lower than that in group c. In addition, it is proved that the products of the interaction between CA and  $\text{Mg}^{2+}$  will not be adsorbed on the quartz surface, and CA has a certain cleaning effect on the quartz surface.



a-quartz b-quartz+Na-Ol c-quartz+Mg<sup>2+</sup>+ Na-Ol d-quartz+Mg<sup>2+</sup>+ CA +Na-Ol

Fig. 9. Fitted spectrum of infrared absorption peak

Table 2. Fitting results of infrared spectrum

Numbering	Peak position	FWHM	Peak area	Sum of peak area
a	2855.5046	25.2140	0.2105	1.0275
	2924.5789	57.0539	0.8170	
b	2856.4120	26.4337	0.2433	1.0637
	2926.1420	49.9792	0.8204	
c	2856.6721	27.4576	0.2775	1.2541
	2926.3558	52.3254	0.9766	
d	2856.0202	26.2461	0.1972	0.8047
	2925.1355	52.1348	0.6775	

### 3.5. Solution chemistry calculation

#### 3.5.1. Mg<sup>2+</sup> hydrolysis component calculation

Mg<sup>2+</sup> hydrolysis reaction is as follows:



From  $K_{SP} = [\text{Mg}^{2+}] [\text{OH}^{-}]_2 = 10^{-11.15}$  (Wang et al., 1988), calculate the critical pH value of  $\text{Mg}(\text{OH})_2(s)$ ,  $\text{Mg}^{2+} = 1 \times 10^{-3}$  mol/L, critical pHs = 9.925. Cumulative constant  $\beta_1$ ,  $\beta_2$ , respectively, calculate the lgC of

each component of  $Mg^{2+}$  before and after the critical pH value and obtain the  $\lg C$ -pH relationship of each component of  $Mg^{2+}$ , as shown in Fig. 10.

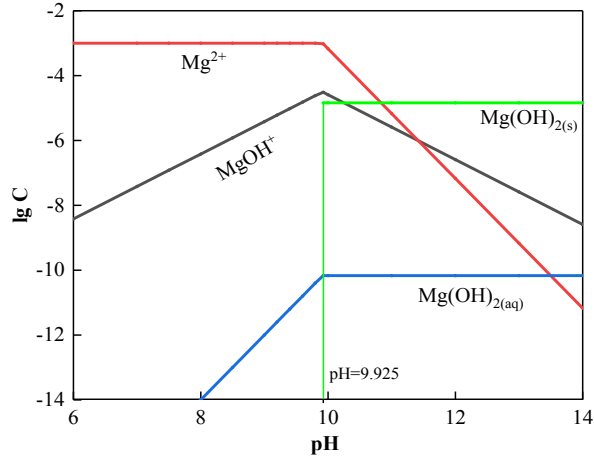


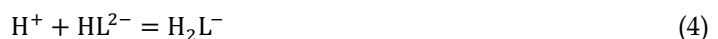
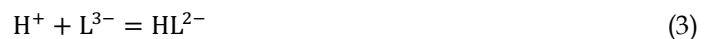
Fig. 10.  $Mg^{2+}$  composition diagram

As shown in Fig. 10, it can be clearly seen that  $Mg^{2+}$  is the main component in the slurry solution; as the pH value increases to weakly alkaline conditions, the concentration of  $Mg(OH)^+$  metal hydroxyl complexes begin to increase. When  $pH > 8$ ,  $Mg(OH)_{2(aq)}$  is formed, but its component concentration is still less than the solubility product of  $Mg(OH)_2$ , not in the form of precipitation; when  $pH \geq 9.925$ , theoretically  $Mg(OH)^+$  starts to be formed  $Mg(OH)_{2(s)}$ , precipitation appeared in the solution, the concentration of  $Mg^{2+}$  began to decrease, the concentration of  $MgOH^+$  also decreased, and  $Mg(OH)_{2(aq)}$  tended to balance.

Comparing the  $Mg^{2+}$  component diagram with the flotation recovery rate under different pH values, the increasing trend of the concentration of  $Mg(OH)^+$  and  $Mg(OH)_{2(aq)}$  components is similar. When the  $Mg^{2+}$  concentration is  $1 \times 10^{-3}$  mol/L, the slurry  $pH = 10$ , the flotation recovery rate is the highest, after  $pH > 10$ , the flotation recovery rate tends to be flat and slightly reduced, in line with the metal hydroxyl complex activation hypothesis.

### 3.5.2 Chelating reaction of CA with magnesium ion

Protonation reaction of CA in water (Wang et al., 1988):



Reacts with  $Mg^{2+}$  to generate complexes at various levels:



The distribution diagram of each component of the product of CA and  $Mg^{2+}$  is shown in Fig. 11. Firstly, CA dissociates, and the primary complexation reaction with  $Mg^{2+}$  occurs to produce  $MgL^-$ , and a very small amount of secondary or tertiary complexation reaction takes place to produce  $MgHL$  and  $MgH_2L^+$ .

The relationship between the distribution of the various components produced and the flotation recovery rate can be seen compared to each other. The  $Mg^{2+}$  distribution curve shows a decrease, which is similar to the recovery rate of the suppression experiment. The generated  $MgL^-$  distribution curve shows an upward trend. From the perspective of chemical reaction equilibrium, when CA dissociates,  $L^-$  interacts with  $Mg^{2+}$  to generate  $MgL^-$ . Due to the first-order complexation reaction, the amount of  $Mg^{2+}$  in the slurry solution system is reduced, which causes the balance of the following two hydrolysis reactions to be changed.



The quantity of  $\text{Mg(OH)}^+$  and  $\text{Mg(OH)}_2$  decreases, so the main components of activated quartz reduce, and the activation effect is inhibited. As a result, the flotation recovery rate decreases, and the inhibition of CA is realized.

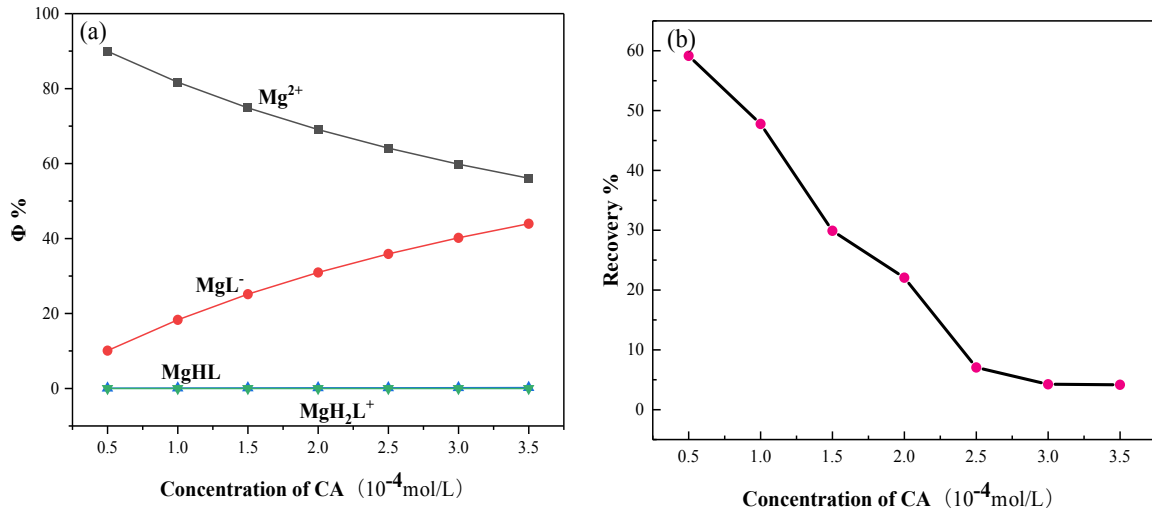


Fig. 11 (a). Distribution of CA and  $\text{Mg}^{2+}$  product components; (b). Effect of CA concentration on the flotation

### 3.6. Schematic model of activation and inhibition process

A schematic of the activation and inhibition process is drawn based on the above experimental findings.  $\text{Mg}^{2+}$  is adsorbed on the surface of quartz through electrostatic adsorption (or physical adsorption), and this adsorption is reversible.  $\text{Mg}^{2+}$  chemically reacts with CA, and the resulting product is magnesium citrate. This product will desorb from the quartz surface and can no longer be adsorbed on the quartz surface.

The activation effect is that  $\text{Mg}^{2+}$  can be adsorbed on the quartz surface, and sodium oleate is adsorbed on the area where  $\text{Mg}^{2+}$  is adsorbed.  $\text{Mg}^{2+}$  acts as a medium, and sodium oleate indirectly completes the adsorption.

The inhibitory effect is that CA reacts with  $\text{Mg}^{2+}$  adsorbed on the quartz and desorbs from the surface of the quartz. Sodium oleate thus loses the medium of adsorption.

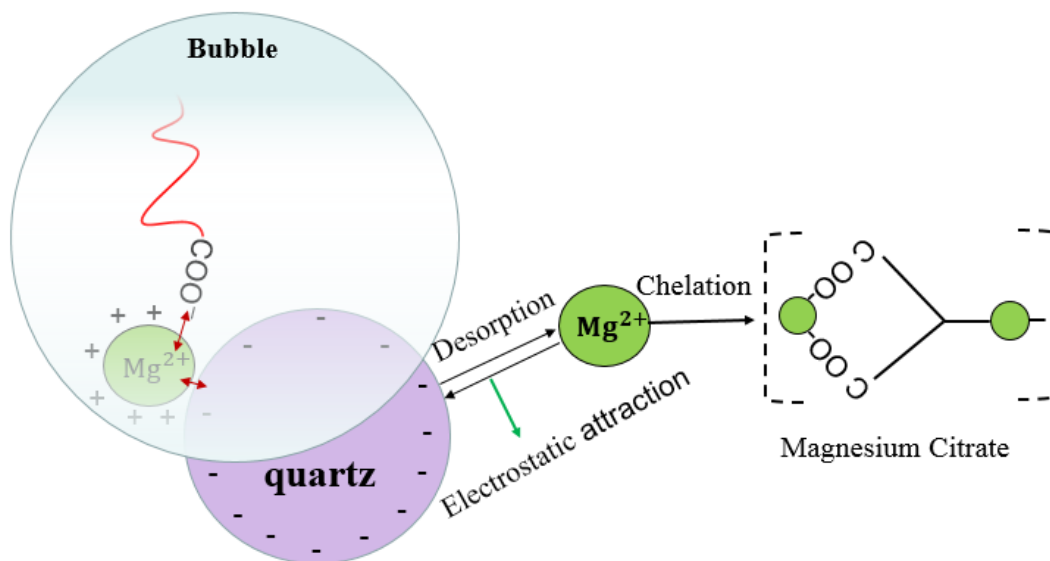


Fig. 12. Schematic of activation and inhibition process

#### 4. Conclusions

Under acidic conditions, the effect of  $Mg^{2+}$  activated quartz is not clear. In an alkaline environment,  $C_{Na-OI} = 120 \text{ mg/L}$ ,  $C_{Mg^{2+}} = 1 \times 10^{-3} \text{ mol/L}$ , quartz obtains the best activation effect, only adds  $2.5 \times 10^{-4} \text{ mol/L}$  of CA can achieve the best inhibitory effect.

The surface of quartz is negatively charged, and  $Mg^{2+}$  is added to it. It is adsorbed on the quartz surface by electrostatic force so that the area where  $Mg^{2+}$  is adsorbed is positively charged, and the zeta potential is significantly increased. This area provides an active site, which acts through electrostatic adsorption. Combine with oleate to realize the floating of quartz. The addition of CA causes the  $Mg^{2+}$  that has been adsorbed on the quartz surface to react with the  $-COOH$  in the CA, and the resulting product desorbs from the quartz surface, causing the positively charged area of the quartz to become negatively charged, the zeta potential decreases, and the oleate loses its point of action. The recovery rate significantly decreased

FTIR qualitative analysis proved that after activation, sodium oleate was adsorbed on the surface of the quartz, and no noticeable chemical adsorption characteristics were found, all of which were physical adsorption. The quantitative analysis results show that the reaction product of CA and  $Mg^{2+}$  is completely desorbed from the surface of the quartz. Therefore, it can be stated that  $Mg^{2+}$  is the medium in which sodium oleate is adsorbed on the surface of the quartz. After CA is added, this medium is cut off to make sodium oleate cannot be adsorbed on the surface of quartz to achieve inhibition.

At the same time, the solution chemistry calculation shows that:  $Mg(OH)^+$  is the key component of activated quartz, and the product formed by the reaction of CA and  $Mg^{2+}$  does not affect inhibiting quartz, but the reaction between the two will consume a large amount of  $Mg^{2+}$ , which is sharply reduces the amount of  $Mg(OH)^+$  inactivated quartz.

#### Acknowledgments

This work was supported by the National Natural Science Foundation of China (Grant No. 51764045), Science and Technology Program of Baotou City of China (Grant No. 2019Z3004-5) and Inner Mongolia Natural Science Foundation (2020MS05048, 2020BS05029).

#### References

- FANG, J., GE, Y., LIU, S., YU, J., LIU, CH., 2021. *Investigations on a novel collector for anionic reverse flotation separation of quartz from iron ores*. Physicochem Probl. Miner. Process, 57(1), 136-155
- LIU, Q., GAO, N., DU, Z., LI, J. CHEN, CH., ZHANG, Z., 2017. *Quantitative detection method of infrared spectroscopy based on second derivative spectrum and characteristic absorption window*. Spectroscopy and Spectral Analysis, 37(06), 1765-1770.
- LIU, R., LI, J., SU, W., ZHANG, X., LI, J., MENG, L., 2020. *Comparison of the activation mechanism of  $Ca^{2+}$ ,  $Fe^{3+}$  on quartz by infrared spectroscopy and XPS analysis*, Spectroscopy and Spectral Analysis, 40(06), 1876-1882.
- M.C. FUERSTENAU, A. LOPEZ-VALBRVIESO, D.W. FUERSTENAU, WANG BOWEN. 1989. *The influence of hydrolyzed cations on the natural hydrophobicity of talc*, Foreign Non-metallic Minerals, 18-21.
- WANG YUBIN, WEN KAN, WANG WANGBO, 2019. *The inhibitory mechanism of citric acid on the floatability of muscovite*. The Chinese Journal of Process Engineering, 19(02), 338-344.
- WANG, D., HU, Y., 1988. *Flotation solubilization*, 138-142, 285-287.
- WENG, S., XU, Y., 2010. *Fourier Infrared Spectroscopy Analysis*. 394-395.
- WHITE, A.F., BRANTLEY, S.L. 1995. *Chemical Weathering Rates of Silicate Minerals*. De Gruyter, 12-15.
- WU, W., SUN, CH., ZHU, Y., .2007. *Inhibition of organic chelating agents on activated quartz and its mechanism of action*. Metal Mine, 02, 33-37.
- YIN, R., CHEN, L., HOU, Q., YUAN, Y, LIU, T., 2013. *Study on the mechanism of magnesium ion activated quartz flotation*. Functional Materials, 44(15), 2193-2196.
- ZHIQIANG, ZHANG, CH., DUAN, S., 2019. *Study on the activation mechanism of  $Mg^{2+}$  on sodium oleate capture quartz*. Metal Mine, 5, 84-87.